Technical Memorandum

To: Dave Bryant, Buyer Group International Inc.

From: Hard Rock Consulting, LLC

Date: December 14, 2023

RE: Shambhala Project – 2023 Field Exploration Assay Results, Geostatistics, and Interpretations

---

As requested by Buyer Group International Inc. ("BYRG"), Hard Rock Consulting, LLC ("HRC") conducted a surficial field exploration program at the Shambhala Project (the "Project") in Albany County, Wyoming, in late June through early July 2023. This memo summarizes the exploration activities carried out by HRC and presents geochemical and geostatistical analyses conducted on assay data returned from American Assay Laboratories in Sparks, Nevada, in late 2023.

Overview

The Shambhala Project encompasses approximately 2.65 square miles of mineral rights in the New Rambler Mining District of Albany County, Wyoming, roughly 50 miles west of the city of Laramie (Figure 1). The Project area is situated within the Medicine Bow Mountain Range and consists of 71 lode mining claims covering portions of Sections 03 through 06, T14NR79W and Sections 19 through 22 and 27 through 34, T15NR79W, on land owned and administered by the U.S.D.A. Forest Service. The approximate geographic center of the Project area lies at 41°13'59" N latitude, 106°17'4" W longitude.

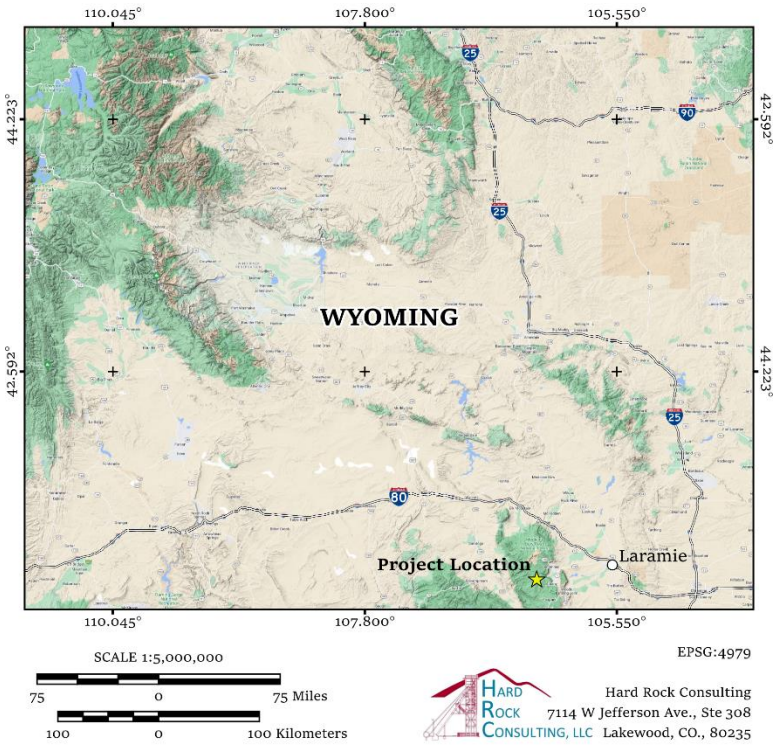

Figure 1 Shambhala Project Location

Physiography in the vicinity of the Project consists predominantly of low-relief upland surface of densely forested Picea-Abies woodland at elevations ranging from 8,700 to 9,700 feet. The Project area is accessible from June through September by WY State Highways 130 and 11 through the town of Albany, and via State Highway 230, which transects the Medicine Bow Mountains just south of the Project. A series of unpaved, gravel roads maintained by the US Forest Service and unmaintained logging roads provide access from state highways to most of the Shambhala Project area.

Regional Geologic Setting

The Archean province of Wyoming contains some of the oldest exposed continental crust in North America, with numerous igneous bodies and tectonic terranes preserving rocks more than 2,500 m.y. old. Following the formation of this ancient crust was a nearly 800 m.y. pause in large-scale igneous activity until what is now modern-day Wyoming experienced scattered mafic plutonism approximately 1,700 to 1,800 m.y. ago (Anderson and Cullers, 1999). The Shambhala Project area falls entirely within the Medicine Bow Mountains, which contain variably deformed lithotectonic blocks bounded by mylonitic shear zones. From north to south and structurally lowest to highest, these blocks are (1) ~2,500 m.y. old Archean crystalline basement and Proterozoic rocks, (2) amphibolite-grade gneiss terrane with rift-related mafic intrusives, (3) a 1,750 to 1,790 m.y. old marginal basin succession of high-grade metasedimentary and meta-volcanic schists intruded by peraluminous granites and minor ultramafic rocks, and (4) a 1,750 to 1,790 m.y. old intermediate to mafic plutonic-metamorphic complex interpreted as the deep roots of an ancient island-arc system (Duebendorfer and Houston, 1987). The region has experienced an extensive and structurally complex tectonic history that can be summarized as intense ductile folding and thrusting during the Paleo- and Mesoproterozoic followed by extension, brittle reactivation, and faulting during the late Cretaceous to Tertiary Laramide Orogeny (Duebendorfer and Houston, 1987).

The Shambhala Project area and central Medicine Bow Mountains are underlain by Paleoproterozoic mafic-to-ultramafic rocks with localized shear zones and deformational heterogeneity. A series of predominantly northeast striking shear zones with subsidiary splays and faults occur across the region (Figure 2). The Mullen Creek-Nash Fork shear zone ("MCNFSZ") is the most notable of these shear zones and constitutes a major Precambrian lineament that separates the Medicine Bow Mountains into two distinct geologic provinces (Houston et al., 1968). Northwest of the MCNFSZ are low-grade miogeosynclinal metasedimentary units ranging in age from 1,650 m.y. to ~2,410 m.y. (Hills et al., 1968). The rocks south of the MCNFSZ are a complex package of metasedimentary schists and gneisses metamorphosed to the upper amphibolite facies 1,750 m.y. ago (Hedge et al., 1967) and younger intrusive rocks that compositionally range from ultramafic to felsic and have been subjected to varying degrees of mylonitic (ductile) deformation (McCallum et al., 1976). It has been postulated that the regionally dominant northeast-striking shear zones were initiated during the latest stage of 1,750 m.y. orogeny and subsequently reactivated through the Laramide Orogeny, approximately 80 to 55 m.y. ago. The rocks exposed in these shear zones comprise a polymetamorphic assemblage ranging from schists to mylonitic gneisses, layered migmatites, and amphibolite-grade meta-mafic units. Regionally retrograded, greenschist-grade cataclasite and mylonite zones also occur and are hypothesized to reflect large-scale brittle deformation associated with the Laramide orogeny (McCallum, 1974).

The MCNFSZ is one of many subvertical, northeast-striking shear zones that collectively define the Cheyenne belt, which serves as the boundary between the Archean Wyoming Province and the Paleoproterozoic Colorado Province in the Medicine Bow Mountains. These shear zones have commonly been interpreted as a Laramide-rotated, Paleoproterozoic mid-crustal thrust system (Karlstrom and Houston, 1984; Duebendorfer and Houston, 1986, 1987; Duebendorfer, 1988), i.e., they were initiated at shallow angles during the Paleoproterozoic, then rotated to their modern steep angles during Laramide extension. Alternatively, Sullivan et al. (2011) proposed that a steeply dipping, stretching series of shear zones formed during the Paleoproterozoic in order to accommodate tectonic shortening through the deformation of the younger, hotter, and mechanically weaker Colorado Province against the older, colder, and more rigid Wyoming Province.

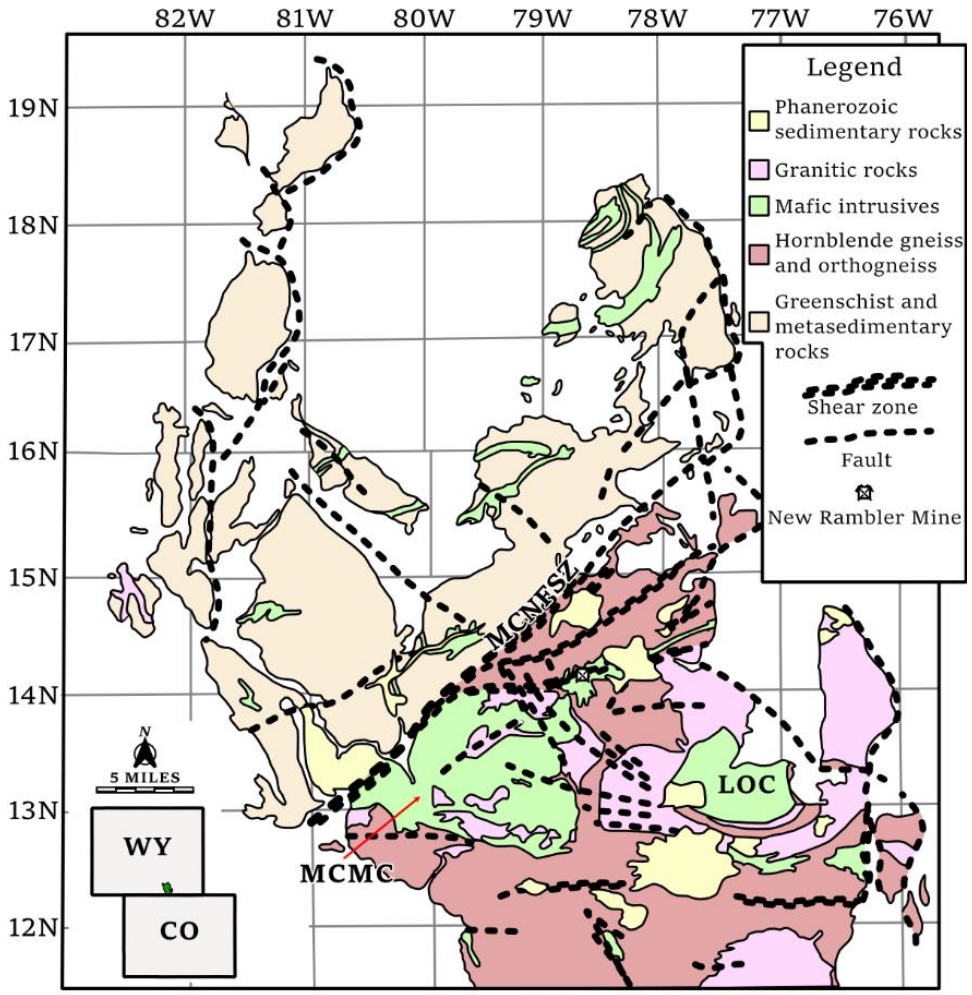

Figure 2 Bedrock Geology of the Medicine Bow Mountains, Albany County, Wyoming (after McCallum et al., 1976). [Map Abbreviations: MCMC = Mullen Creek Mafic Complex; LOC = Lake Owen Complex; MCNFSZ = Mullen Creek Nash Fork Shear Zone]

A zone of mafic plutonic complexes and amphibolitic meta-igneous rocks has been observed and well-documented along a northeastern trend across the Medicine Bow, Sierra Madre, and Laramie ranges (Duebendorfer and Houston, 1986, 1987; Strickland et al., 2004; Jones et al., 2010). Within this zone of meta-mafic rocks, gold-bearing quartz veins and high-grade zones of copper sulfides, and trace nickel and cobalt sulfides, have been locally mined. Most of the base and precious metal mineralization in the central Medicine Bow mountains consists of Au-Cu-bearing, pyritic quartz-carbonate veins that fill southeast-trending tensional cross fractures and faults subsidiary to the MCNFSZ (McCallum et al., 1976).

Field Observations

Local Geology

The local geologic relationships of the Shambhala Project and New Rambler mine areas are obscured by Quaternary gravel and alluvium deposits as well as forest litter anywhere from 6 to 16 feet thick based on observations from prospect pits (Theobald Jr and Thompson, 1969). Densely wooded forests, poor outcrop exposure, and a generally rugged topography, in addition to the high degree of structural complexity preserved

in exposed rocks, makes geologic interpretations for the New Rambler mine area exceedingly difficult. Exposed bedrock in the area is Paleoproterozoic in age (~1,780 to 1,730 m.y. old) and include variably deformed, amphibolitized meta-igneous mafic rocks and weakly deformed monzonitic-to-granitic intrusives (Figure 3).

Figure 3 (A) Massive amphibolite (B) Mylonitic mafic schist (C) Monzonite with feldspar megacryst (D) Weakly foliated monzonite

The oldest rock type in the vicinity of the New Rambler mine is an ultramylonitic biotite-epidote-plagioclase gneiss that is light grey-to-pink, very fine- to medium-grained gneiss composed of oligoclase-andesine feldspar, quartz, microcline, biotite, epidote, and chlorite. In the No. 71 adit, the mylonitic foliation is intense and strikes east-west with a very steep-to-subvertical dip; the rocks exposed in this mylonitic zone are very fine-grained, strongly foliated, and obliquely crosscut by a high-angle fault that is readily observable within the adit (Figure 4). Based on observations from tailings piles and prospect pits, it seems as if historic workings focused on exploiting shear zones like the one exposed in the No. 71 adit, which likely contained quartz-carbonate veins with either Cu, Au, or PGE mineralization.

Immediately surrounding the ultramylonitic biotite-epidote-plagioclase gneiss is a large, structurally complicated, amphibolitized, pseudo-layered tholeiitic intrusive complex known as the Mullen Creek Mafic Complex (Houston, 1968). The Mullen Creek Mafic Complex is largely dominated by medium- to coarse-grained metadiorite and metagabbro consisting primarily of plagioclase, hornblende, and pyroxene with trace magnetite, ilmenite, apatite, titanite, and garnet (McCallum et al., 1976). All mafic-to-ultramafic exposures observed in the field contain chlorite, epidote, and sericite to a certain extent, thereby indicating a retrograde metamorphic event at the greenschist facies, as well as propylitic (hydrothermal) alteration. Exposures of meta-pyroxenite, an ultramafic rock common in layered mafic intrusions, are especially noteworthy and relatively adjacent to the No. 71 adit. Meta-pyroxenite is coarse grained with subhedral-to-euhedral phenocrysts of hornblende and both orthopyroxene and clinopyroxene (which have been altered/uralitized). Iron oxides, namely magnetite, pyrite, and accessory epidote, titanite, apatite, and olivine are also commonly found in meta-pyroxenite.

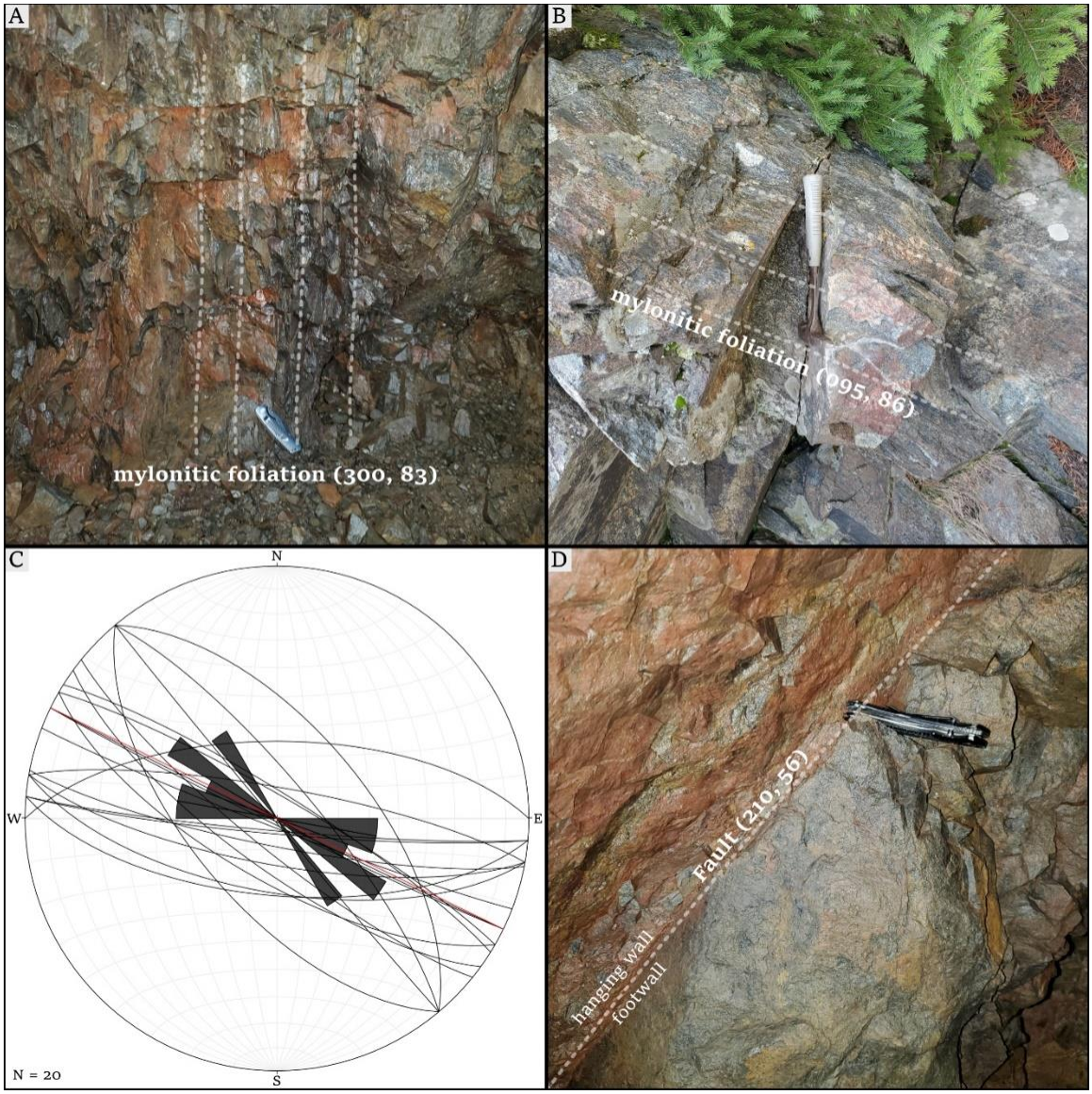

Figure 4 (A) Mylonitic quartzofeldspathic gneiss in adit (B) Mylonitic amphibolite (C) Mylonitic foliation stereonet with mean plane (116, 90) in red (D) Fault with clay-rich damage zone in adit.

In addition to the large masses of intrusive, mafic rocks, the New Rambler mine area also features several small volcanic-to-diabasic dikes and sills, generally less than five feet thick (McCallum et al., 1976). Diabase in the area is fine-to-medium grained and consists of calcic plagioclase and pyroxene. Metamorphosed andesitic-to-basaltic rocks also occur throughout the area.

North of the New Rambler mine area and No. 71 adit are large exposures of monzonitic-to-granitic intrusive rocks with thin, A-type quartz veins and pegmatitic dikes. These felsic intrusives are commonly pink-to-red, medium-to-coarse grained, epidotized, and display rounded weathering patterns. McCallum et al. (1976) presents a detailed mineralogy of these rocks and states that in decreasing abundance, the primary minerals in these granites includes quartz, microcline, albite-oligoclase feldspar, biotite, and chlorite with minor-to-trace amounts of primary epidote, hornblende, muscovite, magnetite, and allanite.

All the units described above display varying degrees of both ductile and brittle deformation including cataclasis, mylonitization/ dynamic recrystallization, and metasomatism/ chemical alteration. The following paragraphs will describe the local structural features of the New Rambler mine and Shambhala claims area.

The dominant structural feature in the Shambhala claims area is a prominent mylonitic foliation that steeply dips and strikes east-west (Figure 5) that McCallum et al. (1976) interpreted as an east-trending splay of the MCNFSZ. The historically mined ore body at New Rambler is localized near the intersection of a poorly defined northeast-striking mylonitic shear zone with the east-west mile-wide belt of intensely sheared rocks and a set of four close-spaced northwest striking fractures (Kemp, 1904; Orback, 1958; McCallum et al., 1976). It is important to note that these features cannot be seen on the surface and are instead documented in historic mine reports. Furthermore, the New Rambler mine workings are currently caved and inaccessible, and nearly all mine records were destroyed in a fire that ended mining activities in 1918, so the following description of the geometry and structural control of the orebody is tenuous at best. The following table presents the known drilling results from the New Rambler area, unfortunately drill collar locations were not available.

Table 1 Historic Drilling Results and Geology from the USBM's 1942 Drilling Campaign

Hole No.	Inclin.	TD (ft)	from	to	Rock type	Alteration	Structures	Pyrite	Description
USBM49-01	-51	270	0	45	diorite				grades into pyroxenite
USBM49-01	-51	270	45	190	pyroxenite	yes			
USBM49-01	-51	270	190	270	pyroxenite			trace	compact from 190 to 270'; small amount of Py from 190 to 200'
USBM49-02	-45	54	0	54	diorite				intersected non-mineralized mine workings at 54.5'
USBM49-03	-65	234	0	50	diorite				grades into pyroxenite and peridotite
USBM49-03	-65	234	50	150	peridotite/pyroxenite	yes	crushed		altered and crushed
USBM49-03	-65	234	150	234	peridotite/pyroxenite			trace	compact from 150 to 234'. Small amount of Py at 200'
USBM49-04	-55	150	0	14	overburden				
USBM49-04	-55	150	14	30	diorite				
USBM49-04	-55	150	30	150	peridotite/pyroxenite	yes	crushed		no mineralization
USBM49-05	-50	174	0	14	overburden				
USBM49-05	-50	174	14	30	diorite				
USBM49-05	-50	174	30	174	peridotite/pyroxenite	yes	crushed	minor	some Py at 160'. Intersected mine workings at 174'
USBM49-06	-65	66	0	14	overburden				

USBM49-06	-65	66	14	30	diorite				
USBM49-06	-65	66	30	50	peridotite/pyroxenite	yes	crushed		
USBM49-06	-65	66	50	66	peridotite/pyroxenite	yes	gouge	minor	some Py and gouge from 50 to 66'
USBM49-07	-45	276	0	50	overburden				
USBM49-07	-45	276	50	276	diorite/pyroxenite	yes			Several altered, sandy horizons contain copper carbonate staining
USBM49-08	-45	148	0	148	peridotite/pyroxenite				Surface debris grades into pyroxenite and peridotite. Small amount of copper carbonates from 70 to 80'. Old workings encountered at 148'
USBM49-09	-50	181	0	181	diorite	yes	pyroxenite lenses		Altered diorite and lenses of pyroxenite the full depth of the hole. Stains of copper carbonate in some pyroxenite lenses
USBM49-10	-45	306	0	65	overburden				
USBM49-10	-45	306	65	100	diorite	silicification	quartz veins		Silicified diorite w/ dark Qtz stringers 65 to 100'
USBM49-10	-45	306	100	306	diorite	yes		trace	small amount of Py at 292'

The New Rambler orebody consists of three large, irregular ore bodies with complicated contacts and sharp lithologic gradients. Kemp (1904) indicates that these pods lack a consistent trend and mineralization is hosted in highly weathered, deformed, and mafic-to-ultramafic meta-igneous rocks at the intersection of a northeast striking shear zone, an east-west striking mylonitic shear zone, and northwest striking faults of moderate dip and significant fault gouge with secondary copper mineralization (Orback, 1958). Diamond drilling has shown that the primary host rocks are metadiorite and metagabbro that gradually grade into pyroxenite and peridotite at inconsistent depths (Table 1; Kasteler and Frey, 1949). The uppermost ore pod is described as domical and extending from 30 to 70 feet below the surface with a horizontal diameter of approximately 40 feet (Kemp, 1904). The upper zone of this body is gossanous and extensively copper leached, whereas the lower part of this oxidized pod contains copper carbonates, sulfates, oxides, hydrates, native copper, and minor copper sulfides near its base. About 50 feet southeast of the oxidized ore pod, a separate sulfide pocket with gradational contacts exists at a depth of approximately 100 feet. This sulfide pocket is 25 feet thick, 30 feet long north-south, and 50 feet long east-west. Immediately west of this pod is another irregular ore pocket of similar dimensions but a different gangue mineralogy more dominated by jasperoid as opposed to quartz and calcite (Kemp, 1904; McCallum et al., 1976). A schematic diagram of PGE, Au, and Ag variability with depth is shown in Figure 5.

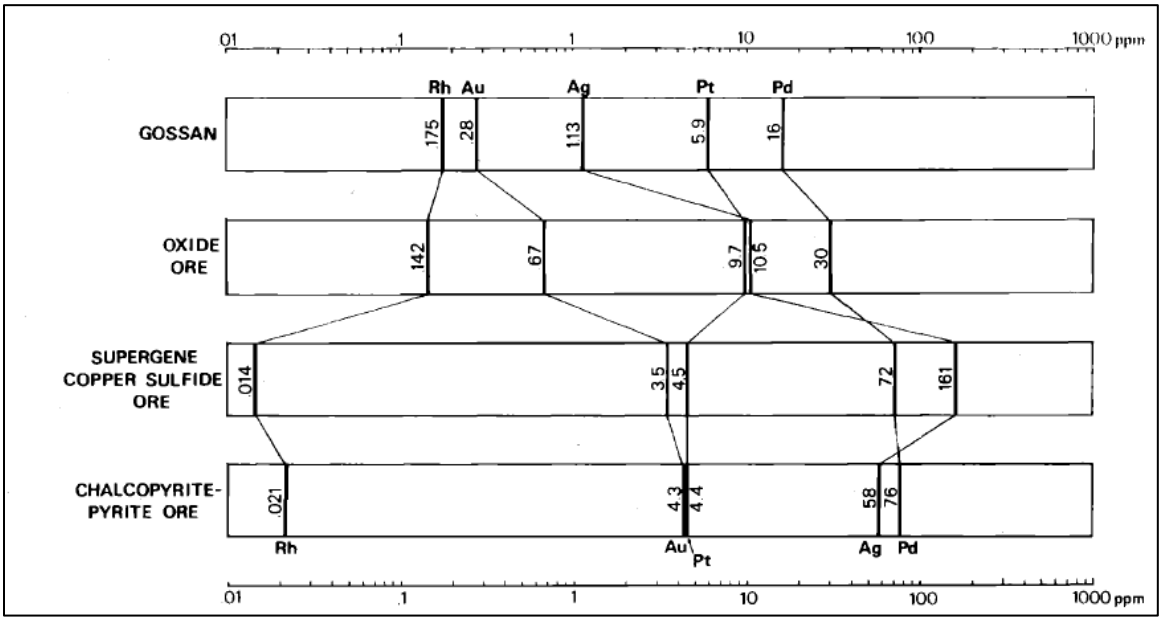

Figure 5 Schematic vertical section of the New Rambler PGE deposit showing average metal contents (ppm, log scale) between weathering profile horizons (McCallum et al., 1976).

Tens of feet east of the three irregular ore pods, underground working encountered quartz-calcite fissure veins (i.e., tensional fractures) related to the four small northwest-striking faults. The US Bureau of Mines (1942, p. 4) indicate that mine development spent a decade focusing on fissure veins under the false assumption that the orebody was hosted along them. Nonetheless, these three ore pods, despite their structural complexity with regards to one another, were responsible for all the historic production at the New Rambler mine.

Mineralization and Alteration

The following descriptions are from the McCallum et al. (1976) study of rocks from the New Rambler Mine's tailings pile. A combination of poor surficial exposure and inaccessible mines makes tailings piles and prospects the best means of studying the geology of the New Rambler Mine area. The New Rambler deposit displays

extensive and intense oxidation-related zoning due to deep weathering and supergene mineral formation. As based on the least oxidized and weathered portions of the deposit, the primary magmatic sulfide ore can be divided into three distinct mineral associations:

(1) An assemblage with primarily pyrite and major magnetite with trace chalcopyrite, pyrrhotite, and pentlandite; occurring as massive sulfides and disseminations in a quartz-sericite wall-rock alteration facies;

(2) An association of chalcopyrite and pyrrhotite with minor pyrite and trace sphalerite, pentlandite, electrum, and various Pd and Pt minerals; occurring as massive sulfide with nodular and granular disseminations in metagabbro; and

(3) An assemblage like (2) in both major ore and gangue mineralogy, but with a unique accessory base and precious mineral suite of sphalerite, magnetite, pentlandite, electrum, and many Pd and Pt minerals.

Assemblage 1 constitutes approximately 5% of the mined deposit (McCallum et al., 1976). This assemblage is dominated by medium-grained magnetite with variable grain shapes and extensive alteration as well as pyrite. Petrographic investigations of Assemblage 1 by McCallum et al (1976) revealed the presence of abundant microscopic sulfide inclusions in pyrite. These inclusions primarily consist of chalcopyrite and pyrrhotite with trace pentlandite. Spectrographic trace element analyses of Assemblage 1 pyrite indicate up to 3,000 ppm Co and up to 1,500 ppm Ni, with disseminated pyrite containing up to 1 wt. % nickel.

Assemblage 2 makes up approximately 80% of the New Rambler deposit and commonly displays pervasive supergene alteration. Ore minerals in Assemblage 2 consist principally of chalcopyrite, pyrite, covellite, and limonite and occur as large, up to fist-sized, sulfide nodules in a jasperoid matrix and as granular and disseminated in quartz (McCallum et al., 1976). Chalcopyrite is the most abundant primary sulfide in Assemblage 2 and is coarse to very coarse with abundant inclusions, including pyrrhotite, mackinawite, and sphalerite. Chalcopyrite also commonly shows variable degrees of replacement by covellite, digenite, and trace chalcocite, as well as supergene alteration to villamaninite, a rare Cu, Ni, Co sulfide. In addition to chalcopyrite, primary pyrrhotite is a major constituent of Assemblage 2, however supergene processes have largely altered primary pyrrhotite to secondary, Ni-rich Co-poor pyrite with Ni greater than 5,000 ppm and Co less than 700 ppm. Further electron probe microanalyses by McCallum et al (1976) indicate that Ni is not homogeneously distributed across secondary pyrite grains, with ranges from less than 0.5 wt. % to more than 2 wt. % between grains. The hypogene platinoid mineral suite of Assemblage 2 consists of rhodian sperrylite [(Pt, Rh)As_2], merenskyite [(Pd,Pt)(Te,$Bi)_2$], kotulskite [Pd(Te,Bi,Sb)], michenerite [(Pd,Pt)(Bi,Sb)-Te], and several unidentified platinoid minerals of various chemical structures. These minerals occur as very fine, anhedral grains enclosed in chalcopyrite or derivative covellite and limonite in secondary pyrite-marcasite-limonite masses (ex-pyrrhotite) and in supergene silica that replaced metagabbro silicates. Electrum is a rare trace mineral in Assemblage 2 and occurs as very fine grains enclosed in jasperoid, merenskyite, and other sulfides. Some of Assemblage 2 is cataclastic and/or veined by supergene pyrite, marcasite, and quartz, but there is limited evidence for primary sulfide recrystallization of hydrothermal mineralization, thereby indicating that cataclasis is likely related to Laramide or Tertiary tectonic forces (McCallum et al., 1976).

Assemblage 3 is about 15% of the New Rambler deposit and shows similarities to Assemblage 2 in terms of major ore mineralogy, however the accessory minerals, textural features, and weathering characteristics are distinctive. Much like chalcopyrite of Assemblage 2, chalcopyrite in Assemblage 3 also contains abundant inclusions, most notably of pentlandite and violarite, likely derived from the supergene alteration of pentlandite. Secondary pyrite and marcasite are major constituents of Assemblage 3, much like Assemblage 2.

Assemblage 3 also uniquely contains pyrrhotite replacement by a wide variety of supergene Cu minerals including covellite, digenite, bornite, and chalcopyrite occurring as very fine grained, concentric, polymineralic masses. Chalcocite, which is rare in Assemblage 2, is the most common supergene product of chalcopyrite in Assemblage 3. Native silver is also documented in Assemblage 3, as fine flakes sparsely dispersed through moderately or poorly crystallized limonite and as larger grains enclosed in secondary calcite in supergene solution cavities. Electrum is also present in Assemblage 3. Two Pt and five Pd minerals make up the platinoid mineral suite of Assemblage 3. Unlike Assemblage 2, michenerite, merenskyite, and kotulskite are rare in this assemblage, which is instead dominated by various platinoid tellurides as well as sperrylite, additionally Assemblage 3 is relatively unaffected by cataclasis.

The metagabbroic host rock in the New Rambler Mine displays three distinct alteration assemblages with varying degrees of silicification, sericitization, chloritization, and sausseritization. Propylitic alteration in the New Rambler deposit is defined by an assemblage of chlorite-epidote-clinozoisite-albite-magnetite-pyrite, and is especially pronounced along shear zones and close to orebodies. Propylitic alteration in the Shambhala Project area is incomplete with remnant hornblende and calcic plagioclase and unaffected biotite. Another prominent alteration assemblage in the New Rambler deposit consists of a quartz-sericite-pyrite assemblage. Pyrite predominantly occurs as veinlets and disseminated grains, and as thin overgrowths on magnetite. Chalcopyrite also occurs as sparse disseminations in quartz-sericite gangue. Silicification and quartz-sericite-pyrite alteration in the New Rambler deposit likely represents nearly barren zones locally developed along the walls of fluid-bearing conduits within the ore body. Most of the New Rambler ore is hosted within the jasperoid alteration zone, where sulfide ore is enclosed in microcrystalline silica that formed during supergene alteration and replacement of the original metagabbroic country rock. There are several varieties of secondary jasperoid replacement in the deposit, ranging from massive microcrystalline quartz to masses of microcrystalline jasperoid that preserve relict textural features of the metagabbroic country rock.

The distribution of ore in the New Rambler deposit strongly correlates with the volume and intensity of hydrothermally altered mafic rock. The structural setting, general spatial relationships between ore and major structures such as shear zones, as well as petrologic textures and predominance of more readily soluble PGE's, such as Pd and Pt, are indicative of a strictly hydrothermal origin of platinoid minerals in the New Rambler deposit. Textures such as sulfide and magnetite fracture fillings, grain boundary infilling, and angular, polycrystalline sulfide aggregate formation in supergene jasperoid indicates preferential replacement of primary mafic igneous minerals with hydrothermal sulfide and platinoid minerals. The intersection of shear zones as well as development of cataclastic zones within the New Rambler deposit enhanced permeability and hydrothermal fluid flow that resulted in base cation leaching from wall-rock and the enrichment of fluids in Cu and PGE's and subsequent mineral precipitation in dilatant space (i.e., as veins or in between grains).

In addition to hydrothermal alteration, weathering and supergene alteration are also critical for the geometry and distribution of precious and base metals in the New Rambler deposit. There are four levels of weathering profile (Figure 6) within the deposit. The basal level consists of supergene pyritization of pyrrhotite and silicification of metagabbro. The second level from the bottom is composed mostly of Cu sulfides with minor pyrite and trace limonite. The next level contains oxidized copper minerals, including malachite, antlerite, brochantite, cuprite, and chrysocolla as well as variably siliceous limonite. The uppermost level is a surficial gossan composed of silicified iron oxides. Microscopic and chemical analyses of New Rambler ore indicate that Pd is not stable in the oxidized upper levels of the deposit. Conversely, Pt is shown to increase in abundance in the oxidized upper zones, as is rhenium.

2023 Surface Exploration

From June 12th to July 1st, 2023, Hard Rock Consulting Geologist Justin Mistikawy and Red Beryl Mining Co. President of Exploration, Steven Cyros, conducted an extensive ground sampling campaign that resulted in 240 total samples including 64 rock samples collected from outcrops, prospect pits, trenches, and mining shafts. The Shambhala claims area is accessible via US Forestry Service maintained dirt trails off French Creek Rd near the Rob Roy Reservoir including US Forest Service roads 500E, 555, 555E, 555F, 559, and 561. French Creek Rd can be accessed through the town of Albany off WY State Highway 11, which connects to WY State Highway 230. Samples were hand collected within Shambhala claims areas. A total of 270 unique localities were visited during this sampling campaign, almost all of which were accessed by foot off trails and gravel roads (Figure 6).

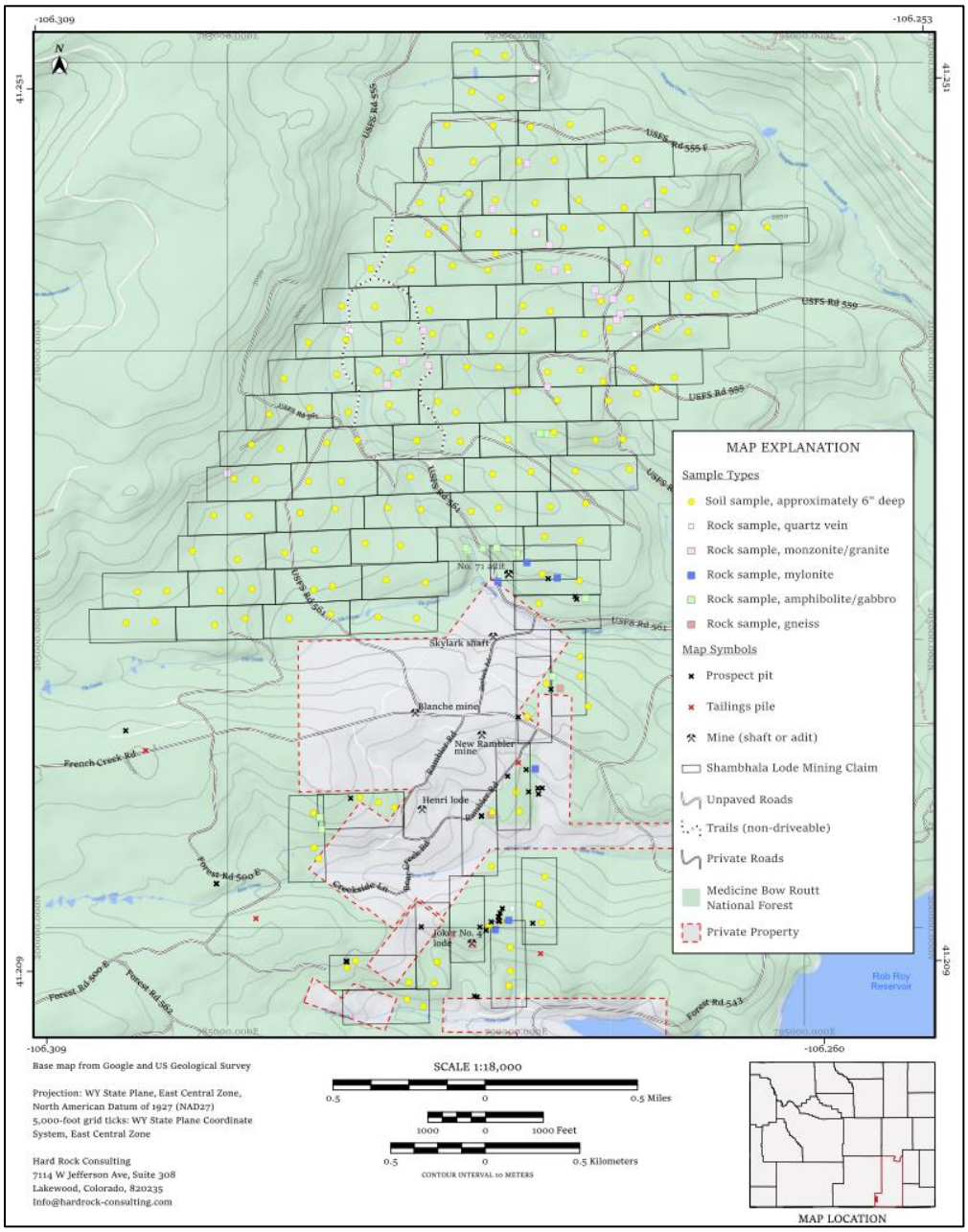

Figure 6 Shambhala Project Minng Claims and 2023 Surface Sample Locations

All sample locations were photographed and geographic coordinates were recorded and stored with FieldMove. Samples of rock were carefully removed from outcrops with a rock hammer or collected from historic prospect pits, trenches, and/or tailings piles, and placed into canvas bags with a Rite in the Rain sample tag. Soil samples (~75 to 300 grams) were taken from a depth of at least 6 inches and placed into plastic bags with a Rite in the Rain sample tag. In addition to the Rite in the Rain sample number, each sample also has a unique Shambhala Project number (e.g., Sh23-001).

Samples of rock and soil were shipped to American Assay Laboratories ("AAL") in Sparks, NV in 5-gallon buckets purchased from Ace Hardware in Laramie, Wy. Soil samples were analyzed for Au via the IO-FAAu30 fire assay method and platinum group elements ("PGE's") via the IM-NF5 method. Rock samples underwent the same tests in addition to IM-4AB26 analysis for non-granitic samples and IM-4AB52 for granitic samples except for samples Sh23-019, Sh23-020, and Sh23-022, which are too small for multiple tests. These samples were only analyzed for Au via IO-FAAu30. All samples were successfully split, prepared, weighed, digested, and analyzed. American Assay Laboratories ensured QA/QC with duplicates, blanks, and standards including: AMIS 682, AMIS 684, CDN-PGMS-22, OREAS 600b, OREAS 905, and OREAS 906.

2023 Surface Exploration Results, Geostatistics, and Analysis

Geochemistry and Geostatistics in Mineral Exploration

Geochemistry and geostatistics are powerful tools for the identification, classification, and exploration of any type of mineral deposits. Significant PGE mineralization commonly accompanies large scale Ni-Fe sulfide mineralization, including pyrrhotite, pentlandite, chalcopyrite, cubanite, and pyrite (Hattori and Cameron, 2004; Barnes and Ripley, 2016). Due to the geochemical properties of PGE's and their affinity for sulfur-bearing minerals and transport complexes, base metals such as Cu, Ni, and Co, as well as precious metals like Au have commonly been used as pathfinder elements for PGE mineralization (Mountain and Wood, 1988; Hattori and Cameron, 2004). It is important to acknowledge that these elements are common in many other types of deposits. Additionally, PGE's, particularly Pd, are highly mobile in acidic waters, much like those produced by the weathering and oxidation of the sulfides common to PGE deposits (Mountain and Wood, 1988). Palladium complexes precipitate to form Pd arsenides, tellurides, antimonides, and sulfides, which are unstable in weathering environments, where they release As, Te, Sb, and S into the ambient environment. These elements and the PGE's themselves are additional pathfinder elements that can be used to explore the potential of significant PGE mineralization in the Shambhala area.

Correlograms are an effective means of visualizing the correspondence between discrete values in a data set, in this case how different elements correspond to one another across soil and rock samples collected from the Shambhala claims area during the 2023 surface sampling campaign (Figure 7 and Figure 8). These plots display the numeric correlative strength between select elements for both soils and rocks on a scale of -1 to +1. These values were calculated via creating a correlation matrix, which contains values that represent the linear relationship between every variable in each set of assay data (Wei and Simko, 2021).

The data utilized in the rock and soil data sets were obtained from AAL in late 2023. Values that were reported below the detection limit were filtered out and reassigned to be half the value of the detection limit. Table 2 presents detection limits as provided from AAL.

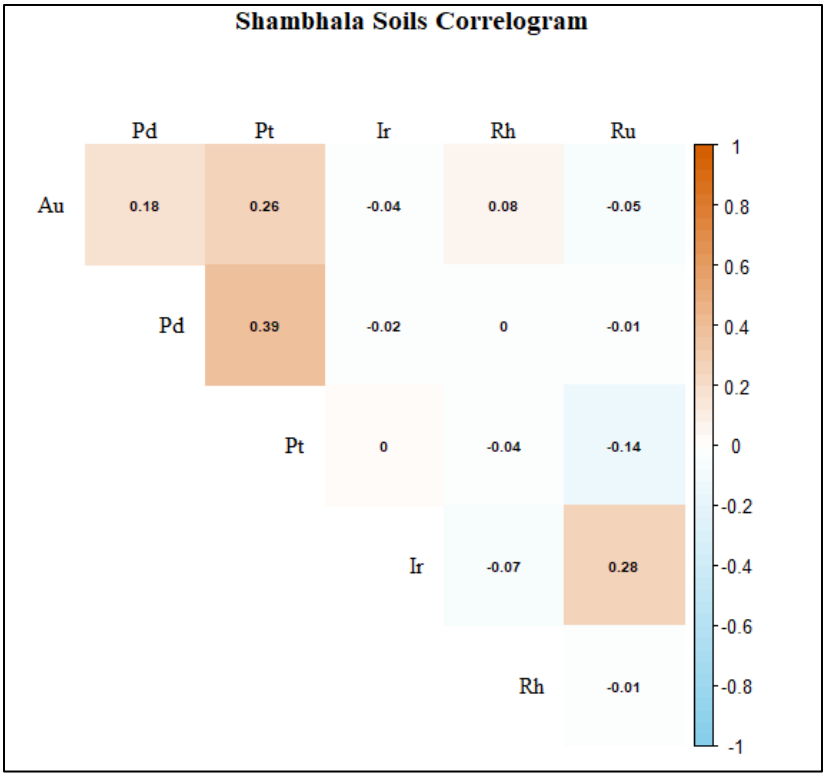

Figure 7 Shambhala 2023 Soil Sample Correlogram

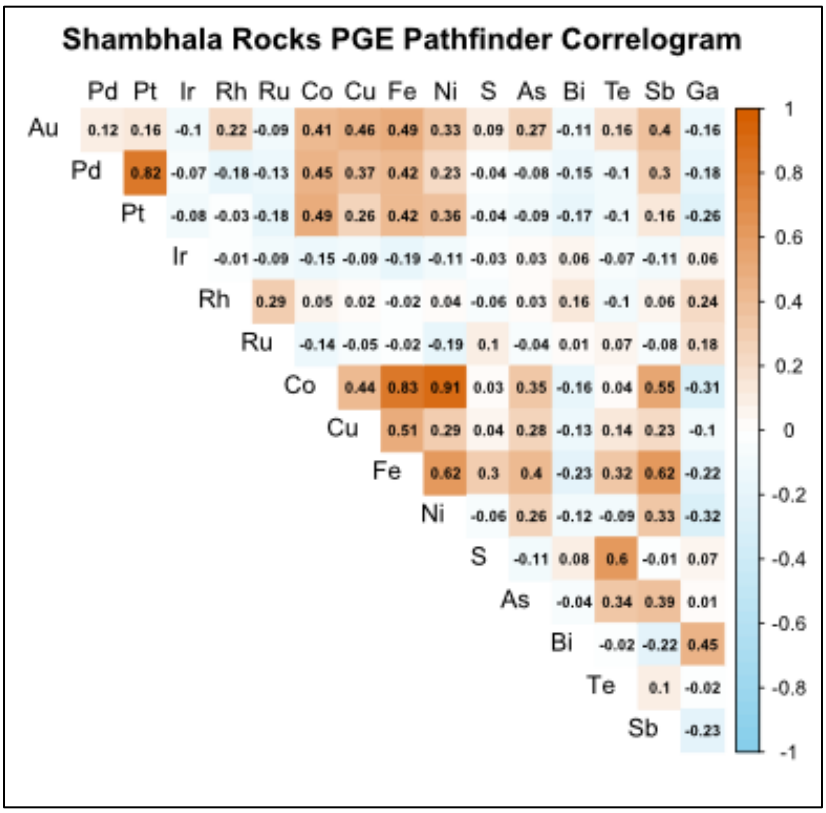

Figure 8 Shambhala 2023 Rock Sample Correlogram

Table 2 PGE Pathfinder Element AAL Detection Limits

Element	Limit (ppm)	Analysis Method
As	0.5	IM-4AB28
Au	0.003	IO-FAPGM30
Bi	0.01	IM-4AB28
Co	0.2	IM-4AB28
Cu	0.5	IM-4AB28
Fe	300	IM-4AB28
Ir	0.001	IM-NF5
Ni	0.5	IM-4AB28
Pd	0.003	IO-FAPGM30
Pt	0.005	IO-FAPGM30
Rh	0.001	IM-NF5
Ru	0.001	IM-NF5
S	30	IM-4AB28
Sb	0.05	IM-4AB28
Te	0.03	IM-4AB28

The Shambhala soil and rock correlograms provided in Figure 7 and Figure 8 indicate high correlative strengths (values greater than 0) between Au, Pt, Pd, and multiple base metals including Co, Cu, Ni, and Fe. The highly chalcophile nature of many of these elements as well as the local geologic context could suggest the presence of sulfide mineralization in the Shambhala claims area. A moderate correlation also exists between base metals and As, Sb, Te, and S, thereby suggesting the weathering of sulfide minerals to unstable arsenides, tellurides, and antimonides (Mountain and Wood, 1988). Notably, Pd, which is highly mobile in the fluids produced by sulfide weathering, does not seem to share a strong correlation with As, Sb, Te, and S. However, Pd has been shown to have significant mobility in surface and near-surface environments (Hattori and Cameron, 2004). Note that Ag has been left off these plots as all analyses were below AAL's IM-4AB28 detection limit (0.3 ppm).

Correlograms are highly effective for visualizing the correlative strength of PGE's and their pathfinder elements, yet, they entirely neglect the spatial dimension of the Shambhala rock and soil assay datasets. In order to visualize the geographic distribution of elements in the samples collected from the Shambhala claims area, several geochemical interpolation maps were produced for elements of interest. All interpolation maps were produced with the gstat package in R Studio (Pebesma, 2004), and then plotted onto an EPSG:3857 georeferenced 40x40m grid created with the sf package in R Studio (Pebesma and Bivand, 2023). The grids represent the bounding box of the samples used to make the interpolation maps.

There are many ways to make interpolation maps, which fundamentally show predicted values at unknown points based on a set of specific mathematical parameters. The two types of interpolations utilized for both soil and rock datasets were Inverse Weighted Distance (IDW) interpolations and Ordinary Kriging. An IDW interpolation computes a predicted value at unknown points by computing a weighted average, where weights are assessed according to their distance from the interpolated or predicted locations. Interpolations created via IDW interpolations are excellent for visualizing hotspots within a dataset, however they do not fill in the gaps as well as Ordinary Kriging interpolations, which use a theoretical mathematical model to predict values at unknown locations given the spatial distribution of data. Therefore, Ordinary Kriging interpolations more

effectively fill in gaps between data points than an IDW interpolation. Creating an Ordinary Kriging interpolation map demands that the observed spatial distribution of data be summarized with a specific type of chart known as a variogram. There are many types of variograms that will be discussed in the following paragraph. Note that some locations in the rock and soil datasets were jittered, or slightly changed, to accommodate Ordinary Kriging, which does not work if there are multiple samples at one location.

Consider the Ordinary Kriging process for Co, which begins with a series of lagged scatterplots. These display data grouped according to their separation distance (Figure 9). Following the lagged scatterplots, variogram clouds were created to plot the difference between pairs of sample values as a function of separation distance. Variogram clouds show all possible squared differences of data pairs against their separation distance (Figure 10). This difference is divided in half to account for the two points that share this value, this is also known a semi-variance or γ, which is simply a measure of dissimilarity between points. The variogram cloud can be used to show the degree of variance of data pairs over distance. The variogram cloud is then plotted over distance intervals to produce a sample variogram (Figure 11). The sample variogram represents the geostatistical data set that spatial correlation or interpolations are often modeled from. Sample variograms by default ignore the directional component of a data set and assume isotropy or direction independence semivariance. A directional variogram was employed to explore the strength of anisotropy in four directions (north, northeast, east, and southeast) (Figure 12). Lastly, the cutoff width, or maximum distance up to which point pairs are considered and the width of distance interval over which point pairs are averaged in bins (Figure 13).

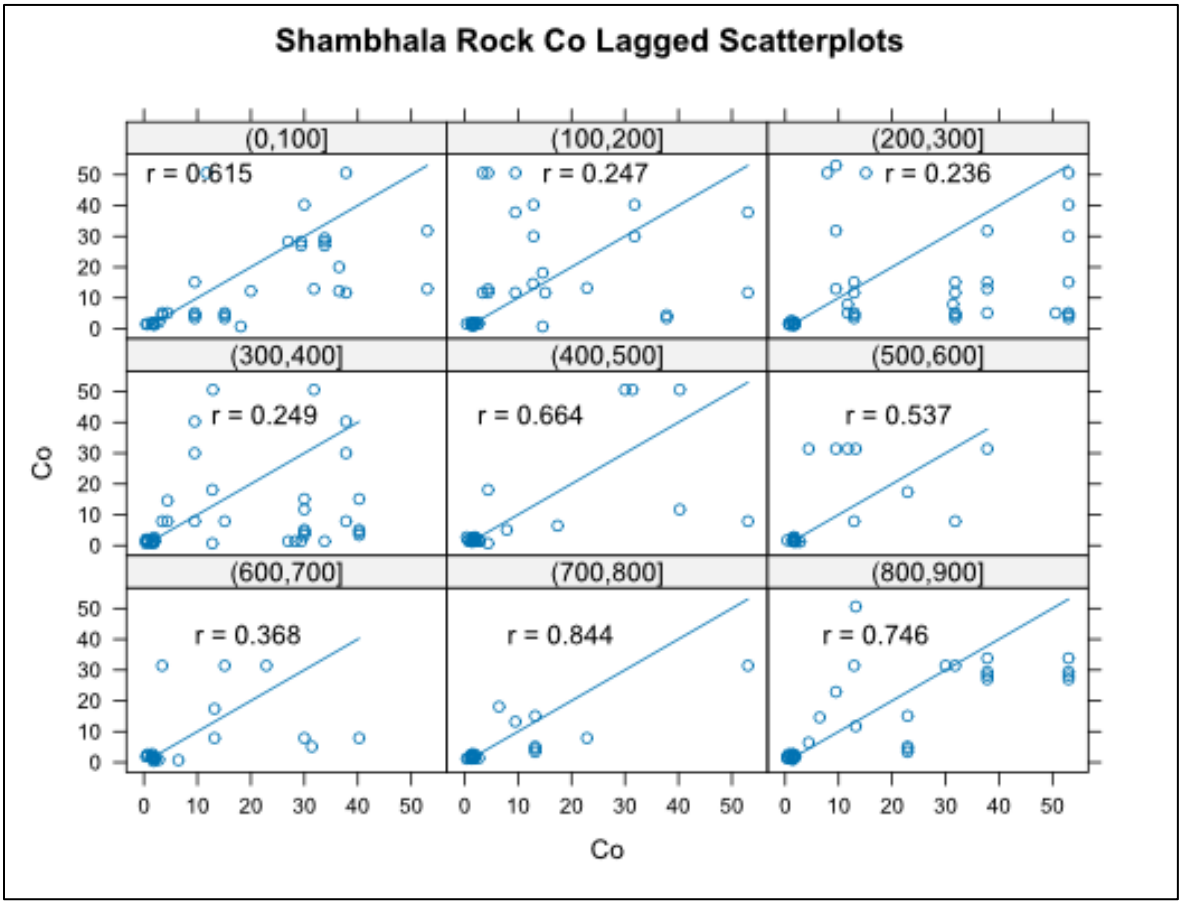

Figure 9 Shambhala Rock Co lagged scatterplot Note that the number on the top of each plot refers to separation distance between pairs and R is the strength of the correlation

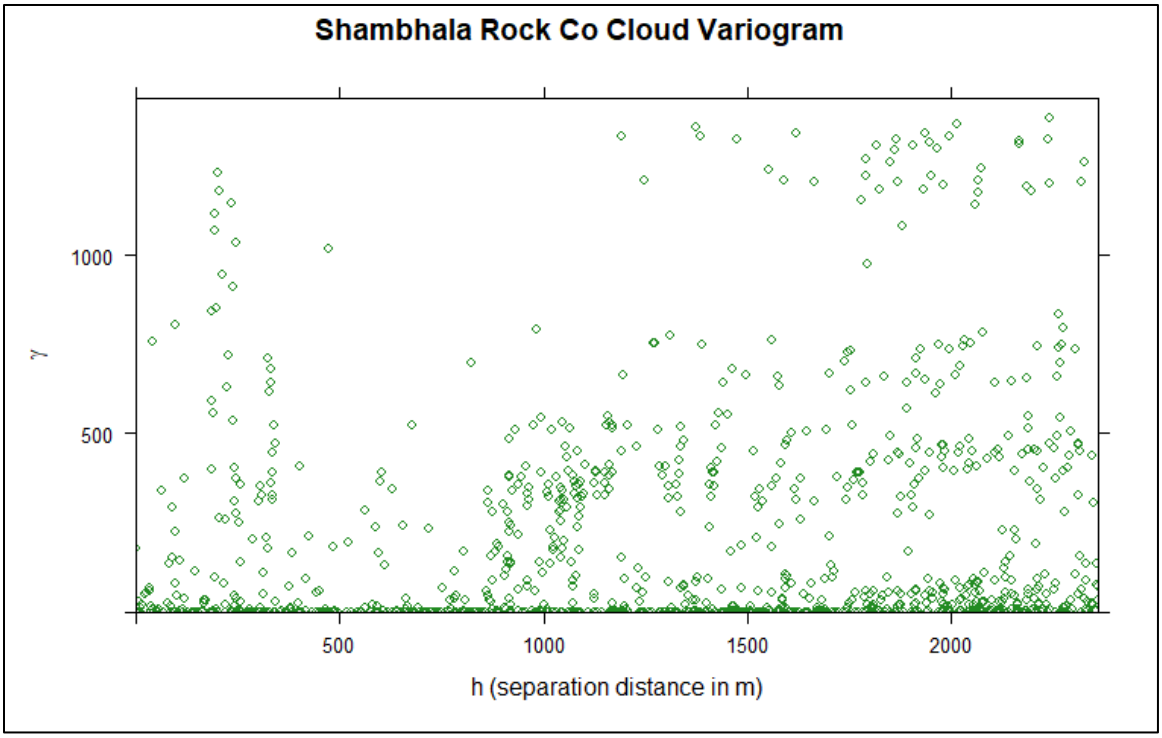

Figure 10 Shambhala Co variogram cloud. Note that γ is semi-variance of Pt

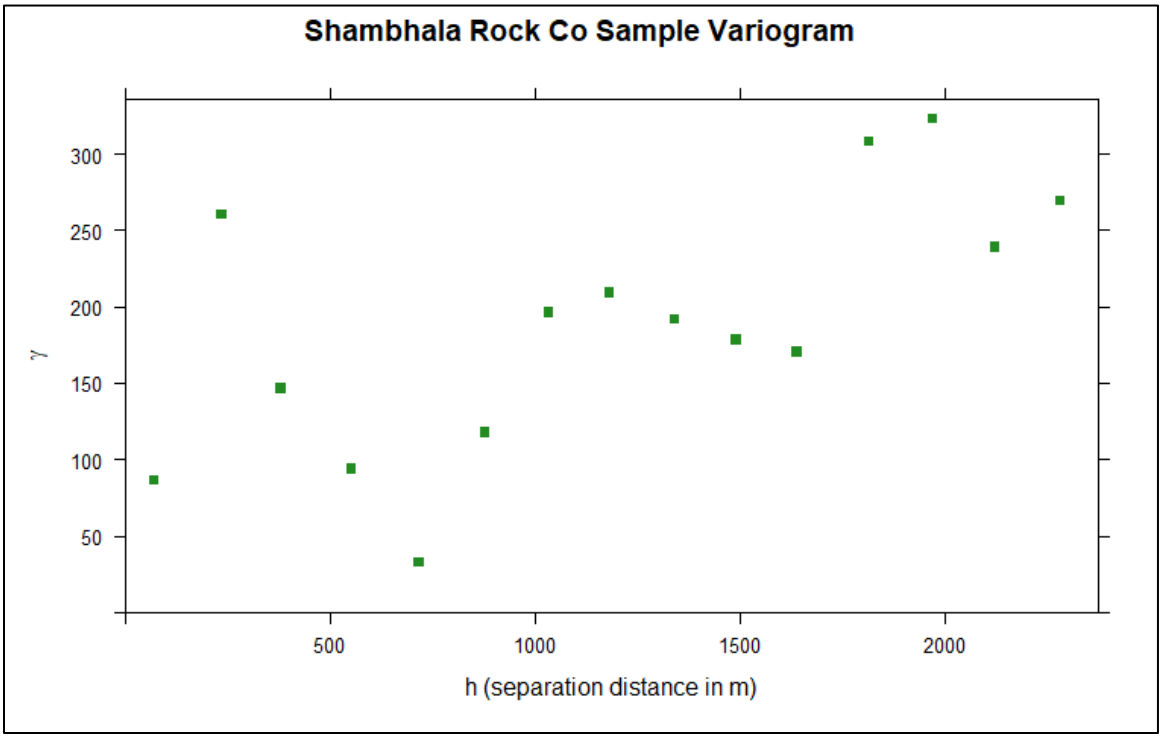

Figure 11 Shambhala Co Sample Variogram. This is what the Ordinary Kriging Theoretical Model is fit to

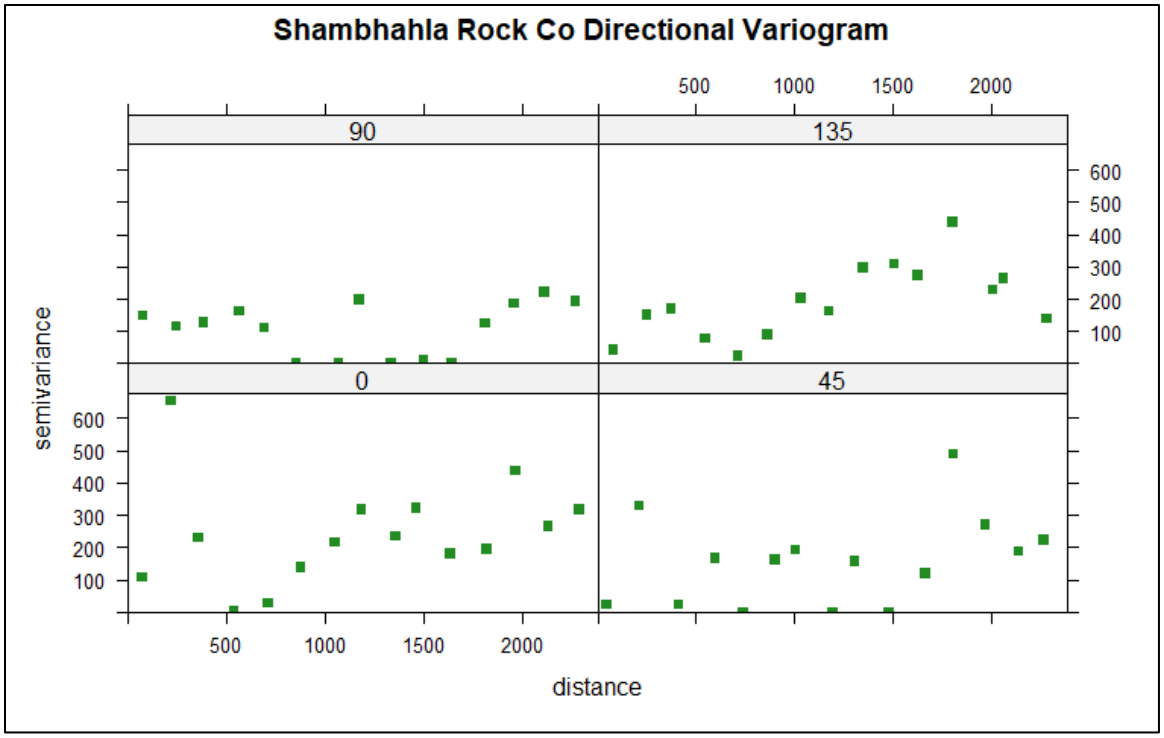

Figure 12 Shambhala Co Directional Variogram for 0° (North), 45° (Northeast), 90° (East), 135° (Southeast)

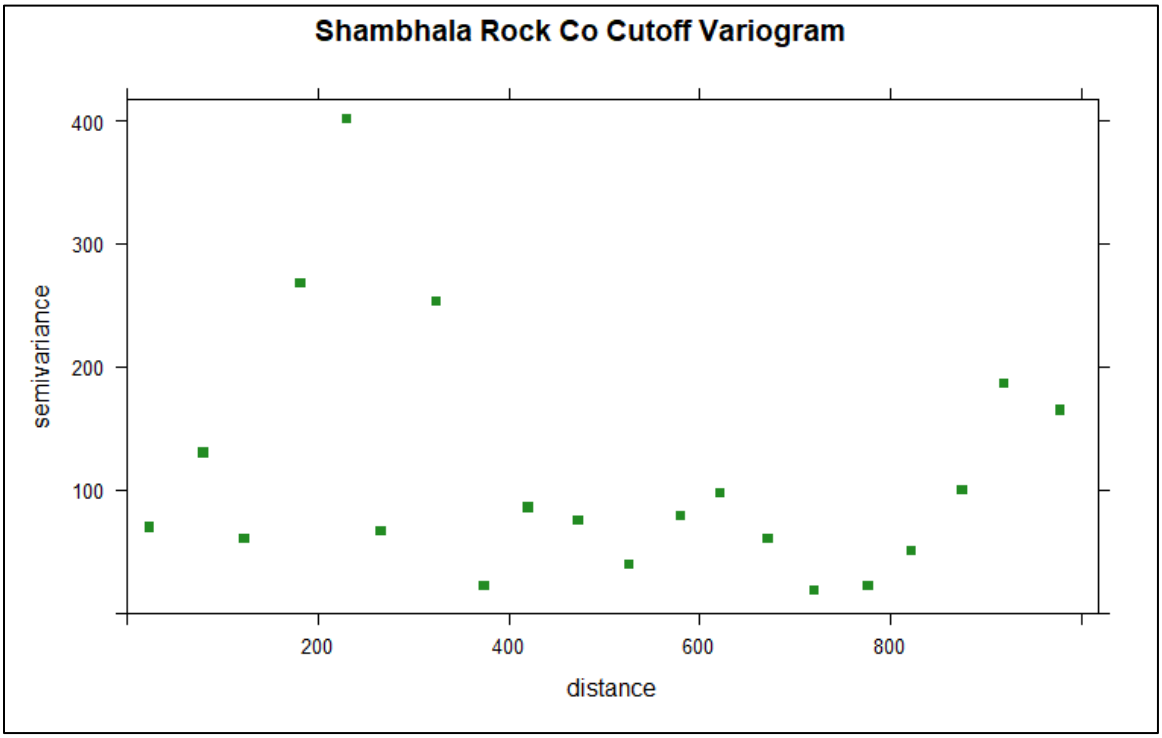

Figure 13 Shambhala Co Cutoff Variogram

Following the determination of the sample variogram, a theoretical mathematical model was tested, best fit, then subsequently added to inform the interpolation (Figure 14). There are many different mathematical model types as well as parameters that can be inputted to force the theoretical variogram to fit the observed or sample variogram. Examples of these mathematical models include Exponential, Spherical, Gaussian, Wave, etc., and important parameters include the nugget and psill values, and range value. Given the limitations of iterative computations, the fit.variogram function was utilized in R studio to return a numerical fit to each sample variogram (Pebesma, 2005). For the Shambhala Rock Co variogram, the numerically determined best fit parameters were for a Wav or Wave type model with a psill value of 107.23023, a nugget value of 96.73686, and range value of 760.5481. For a graphical reference of how well this data matches the observed variogram, refer to Figure 14. Note that some datasets (for example As and Cu) had to be log normalized prior to variogram model fitting because their distribution was impossible to numerically fit a model to.

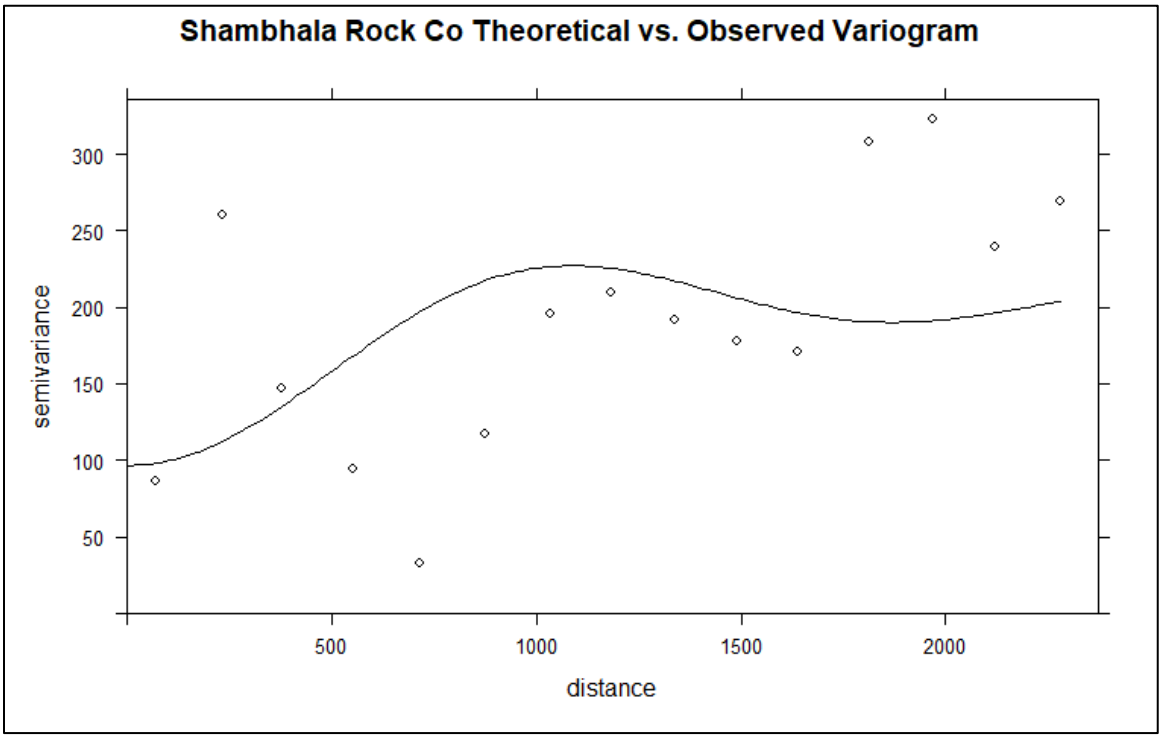

Figure 14 Shambhala Rock Co Observed (circles) vs Theoretical Variogram (solid line)

This workflow was followed for every element analyzed in soil samples (Au, Pt, Pd, Ir, Rh, Ru) and PGE's and select PGE pathfinder elements for rock samples including As (log), Au, Co, Cu (log), Fe, Ga (log), Ni, Pd, Pt, and Rh. Figure 15 displays the differences between the IDW and Ordinary Kriging interpolations for Shambhala Rock Co. As discussed previously, the IDW interpolation effectively highlights where samples had high Co values with limited predictive power away from known locations, unlike the Ordinary Kriging interpolation, which smoothly filled in the interpolated space.

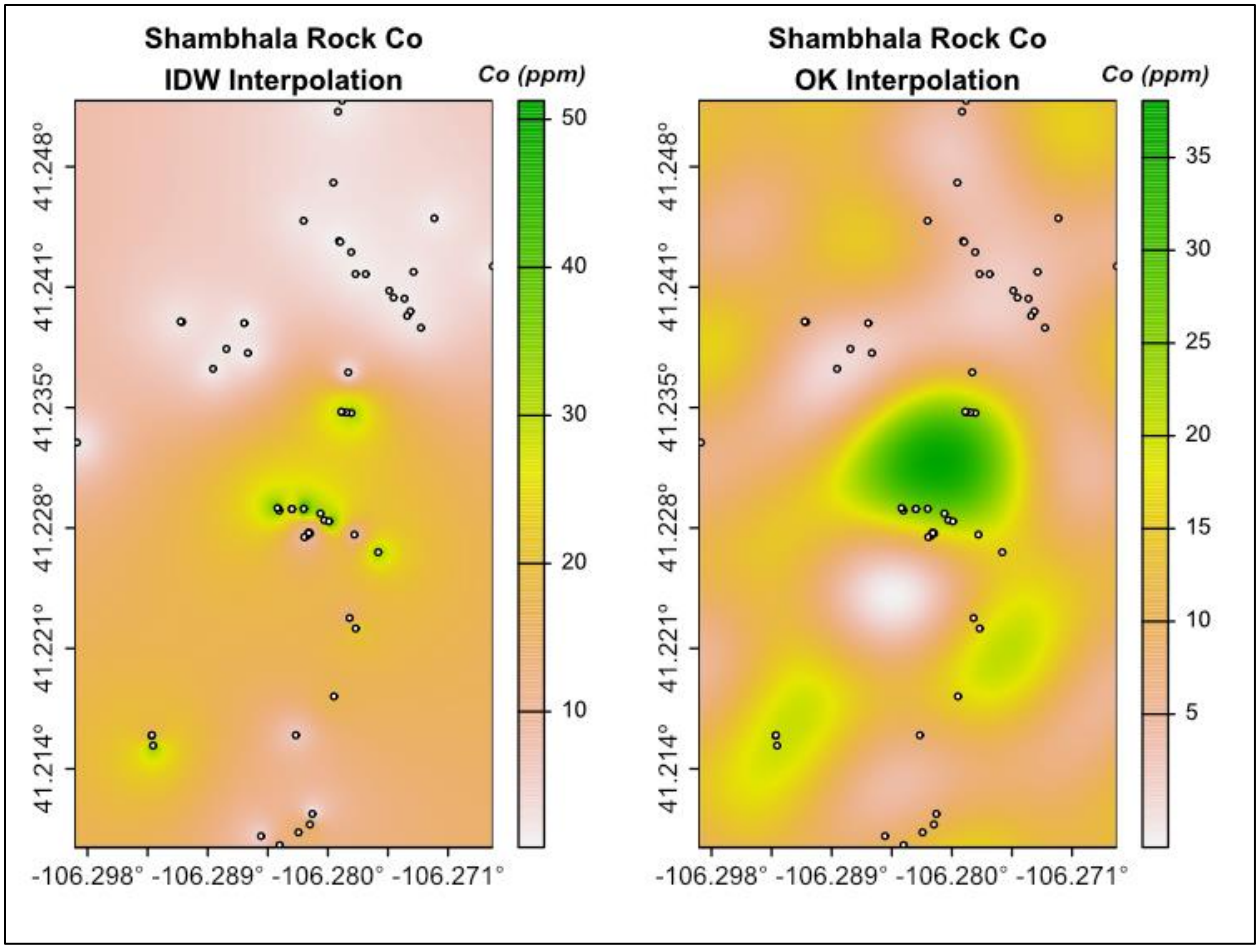

Figure 15 Shambhala rock Co IDW vs Ordinary Kriging (OK) Interpolation maps. White circles are sample spots

Shambhala Geochemical Interpolation Results and Discussion

The 2023 Shambhala surface soil and rock sample Ordinary Kriging interpolations, and to a lesser extent IDW interpolations, revealed several geochemical features of note that may reflect the subsurface geology and mineralization trends of the Shambhala claims area. The rock interpolation maps for several base metals (As, Co, Cu, Ni) share similar trends and apparent hot spots, particularly just north of the No. 71 Adit in claim blocks 37 – 39, 42 – 44, and 47 – 49 (Figure 16). This trend is especially pronounced in As, Co, and Ni and less so in Cu. However, Cu and As also exhibit slightly anomalous values in the southwestern claims area. The main No. 71 Adit anomaly geologically coincides with altered amphibolitic rocks including mylonitic metagabbro and metapyroxenite (Figure 17). The 1942 USBM diamond drilling campaign encountered abundant diorite and metapyroxenite anywhere from 50 to 250 feet, and based on the available publications it is likely that these geologic units, particularly metapyroxenite/metaperidotite, host base + precious/PGE metal veins and were formerly targeted for exploration (USBM, 1942; McCallum et al., 1976). Furthermore, this identified anomaly coincides with a major shear zone present on a geologic map of the Rob Roy Reservoir (Hausel and Sutherland, 2005), and is also observable in the field within the No. 71 adit. The Pt and Pd Ordinary Kriging interpolation maps for both rock and soil samples revealed patterns like those of the rock base metals, with apparent hotspots coinciding in the same geographic area and shear zone with altered mafic rocks (Figure 18). The lack of above baseline Pd levels in the soil sample interpolation map (Figure 8) likely reflects the high mobility of Pd in surface media (Hattori and Cameron).

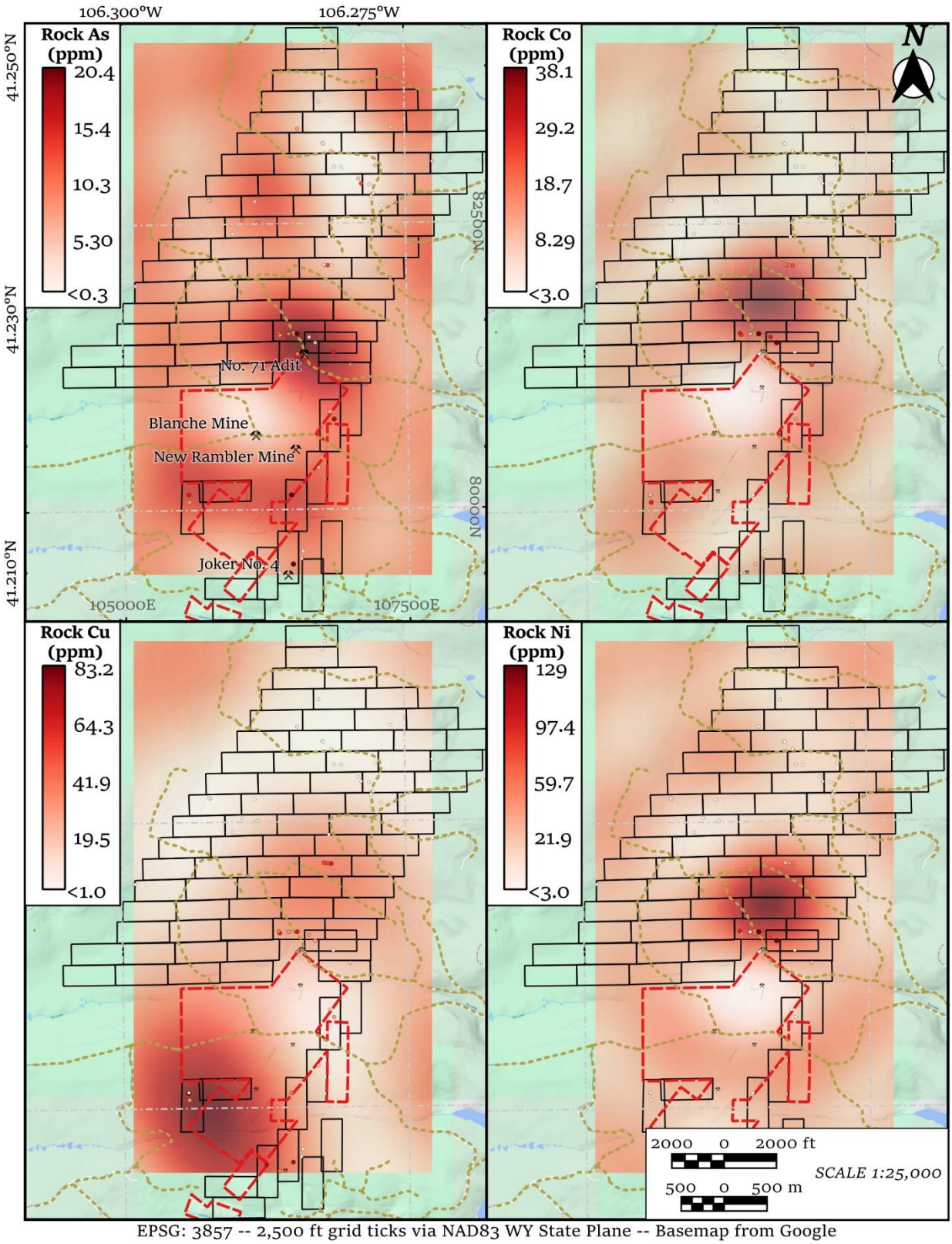

Figure 16 Shambhala rock base metal interpolation maps with claim blocks (solid black) and private property (dashed red). Note that As and Cu interpolations are for log-normalized data.

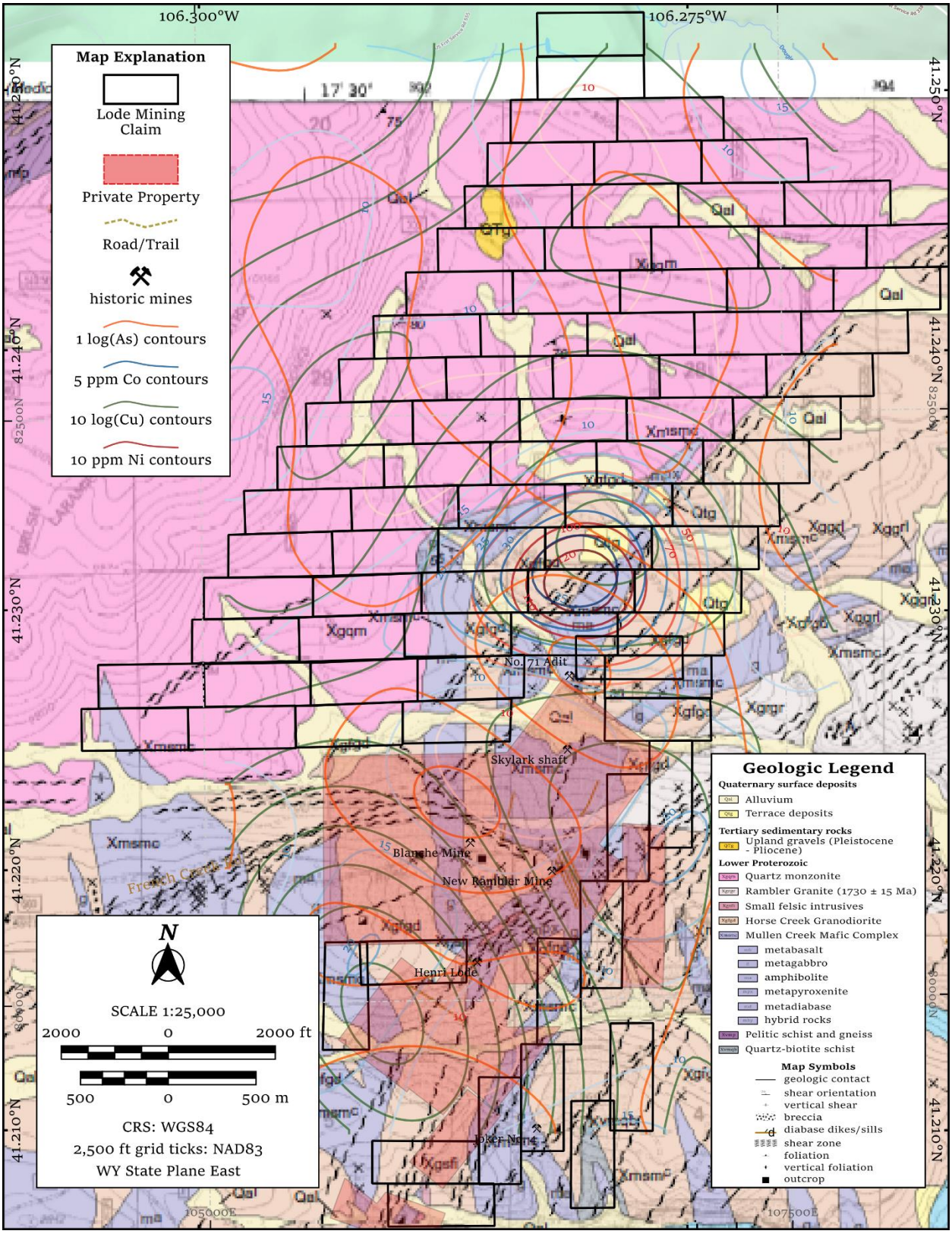

Figure 17 Shambhala rock base metal (As, Cu, Co, and Ni) contours atop a geologic map of the Rob Roy Reservoir area (Hausel and Sutherland, 2005). Note that contours for As and Cu are based on log-transformed interpolations.

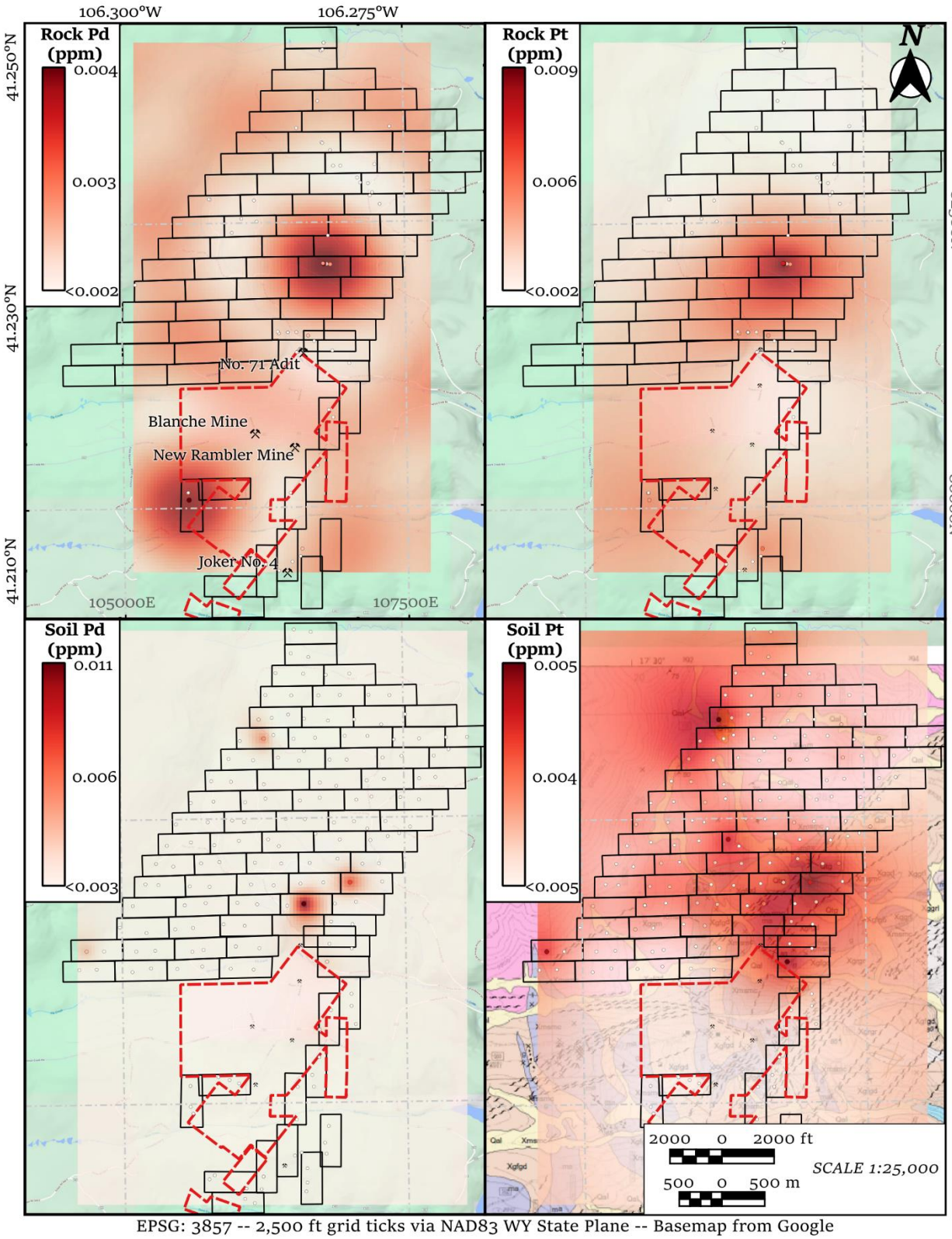

Figure 18 Shambhala rock and soil Pt & Pd Ordinary Kriging Interpolation maps. Soil Pt interpolation map is overlain atop a geologic map of the Rob Roy Reservoir area (Hausel and Sutherland, 2005). Claim blocks are in solid black lines and private property in dashed red lines.

In addition to the base metal and Pt/Pd anomaly, the ordinary kriging interpolation maps also revealed a linear feature that runs roughly southwest-northeast through the northern claims area. This feature is most strongly recognized in the rock Fe ordinary kriging map (Figure 19). Given the geologic context of the area (Hausel and Sutherland, 2005), this feature could either be a sharp geologic contact between deformed and altered mafic-to-ultramafic rocks and younger more felsic intrusives to the northwest; or a structural discontinuity, most likely a shear zone. If this feature represents a shear zone, it is likely that it hosts vein base metal mineralization and potentially PGE mineralization as well. The location of this potential structural anomaly is slightly north (approximately 2,000 feet) of the contact between the locally mylonitic and altered Mullen Creek Mafic Complex and younger, more magmatically evolved and less deformed quartz monzonite. This structural anomaly also may be a continuation of a shear zone presented on the Hausel and Sutherland (2005) geologic map. The intersection of the mapped shear zone with this identified structural anomaly is at approximately located 41.22794, -106.29964. Given the geologic complexity of the area and lack of historical drilling and research, it is impossible to definitively make any conclusions about subsurface geology and/or mineralization.

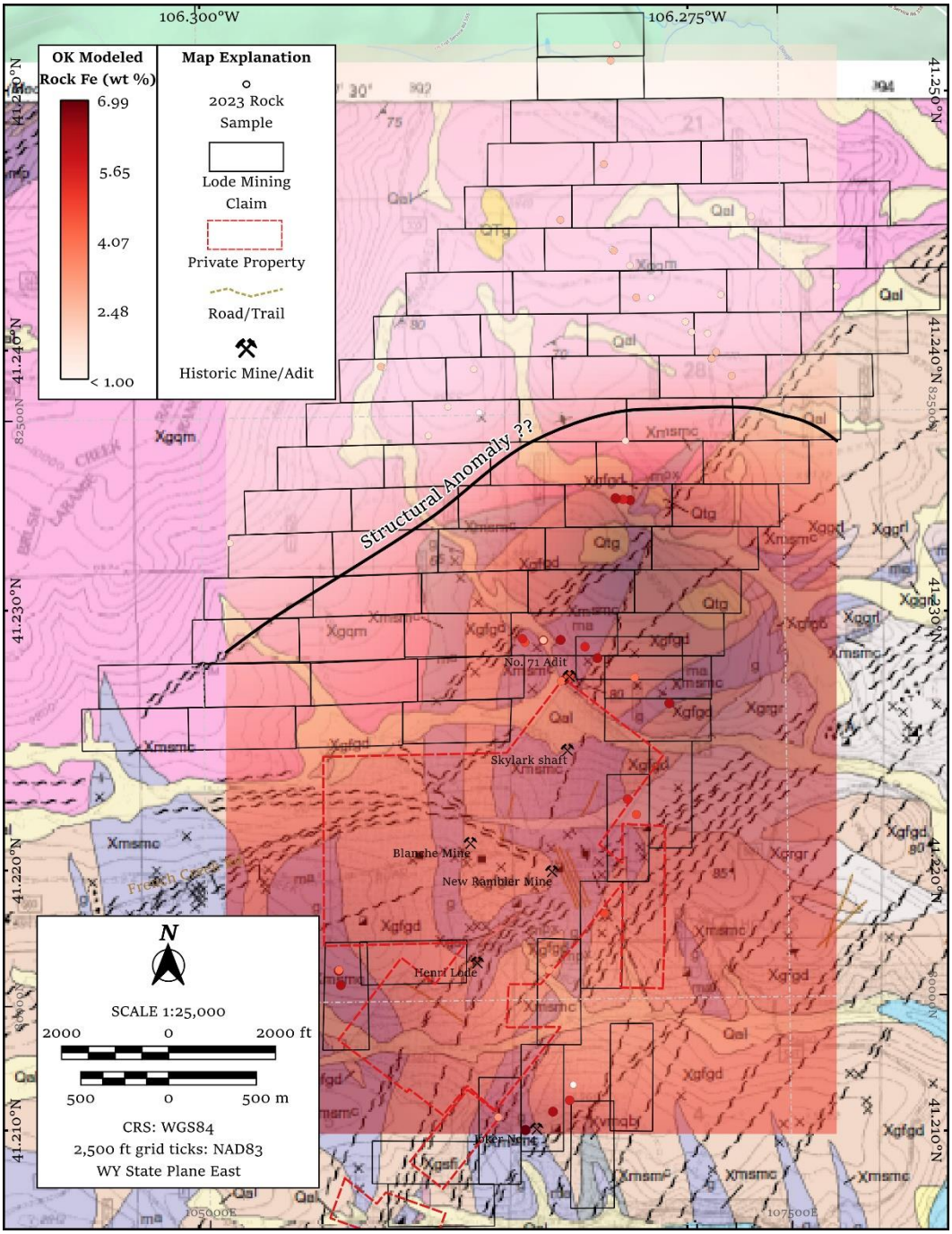

Figure 19 Shambhala rock Fe Ordinary Kriging (OK) Interpolation map with location of interpreted structural anomaly in black line, overlain on geologic map of the Rob Roy Reservoir area (Hausel and Sutherland, 2005)

Preliminary Conclusions

Complexly deformed and altered Paleoproterozoic mafic-to-ultramafic rocks related to the Mullen Creek Mafic Complex underlay the Shambhala project area. Historic mines in the claims area are located at the intersections of mylonitic shear zones and faults in deformed mafic intrusive country rock. The most notable deposit in the area, the New Rambler Mine, consists of three irregular ore bodies. Copper, gold, silver, and PGEs were extracted via underground mining from these three ore pods until a mill fire stopped all operations in 1918.

Surface outcrop exposure is exceedingly poor in the claims area as it is densely forested and covered by thick soil cover (up to 15 feet thick based on prospect pits). Geologic investigation reveals the area to be mostly underlain by amphibolitic metaigneous rocks that irregularly contact gneissic rocks and weakly deformed granitic-to-monzonitic intrusions. Mining shafts and prospect pits in the area are apparently focused on a prominent, roughly east-west striking zone of intense mylonitic shearing. HRC collected 64 rock samples from either in-situ outcrop or prospect pits/tailings piles in addition to 176 soil samples collected from depths of approximately 6 inches. All samples were sent to American Assay Laboratories, Inc., in Sparks, Nevada for multi-element, Au, and PGE assay.

Following geostatistical analyses of the returned surface sample assay data, it is apparent that there are two geochemical anomalies in the Shambhala claims area that merit further investigation: 1) the base metal hotspot centered on altered mafic-to-ultramafic rocks; and (2) a strong discontinuity (best recognized in the Fe Ordinary Kriging interpolation map) that represents a roughly southwestern to northeastern break in geochemistry and geology. This break could represent a shear zone, a sharp contact between older mafic-to-ultramafic rocks and a younger quartz monzonite, or some combination of the two, i.e., a contact that was exploited as a structural weakness upon tectonic forcings.

These identified anomalies are likely worth exploring with refined Phase I sampling and mapping activities. In order to improve interpolation model precision and smoothing, it would be worthwhile to conduct a more-focused, higher resolution (sample spacing = 200 ft) soil sampling program within the identified hot spot area or claim blocks 37 – 39, 42 – 44, and 47 – 49. Furthermore, geologic mapping in that same area at a very fine scale, ~1:5000, could identify and constrain the geometry of shear zones to provide insight into the nature of the structural geochemical anomaly. Lastly, local-to-regional scale geophysics, via either the USGS aeromagnetic survey or local GPR investigations could provide valuable insight into the subsurface geology. Local GPR would be crucial for identifying known historic workings in the claims area while also identifying potential faults or structural discontinuities that could serve as reasonable drill targets. The strong base metal and PGE correlations with the observed and mapped geology are promising with regards to the presence of a PGE deposit. Refined surface sampling and mapping will further aide in the location of structures/areas that are worth exploring with phase 2 activities.

References

Anderson, J. L., and Cullers, R. L., 1999, Paleo- and Mesoproterozoic granite plutonism of Colorado and Wyoming. Rocky Mountain Geol., v. 34, no. 2, p. 149-164.

Barnes, S., and Ripley, E. M., 2016, Highly Siderophile and Strongly Chalcophile Elements in Magmatic Ore Deposits. Reviews in Mineralogy & Geochemistry, v. 81, p. 725-774.

Duebendorfer, E. M., and Houston, R. S., 1986, Kinematic history of the Cheyenne belt: A Proterozoic suture in the southeastern Wyoming. Geology, v. 14, p. 171-174.

Duebendorfer, E. M., and Houston, R. S., 1987, Proterozoic accretionary tectonics at the southern margin of the Archean Wyoming Craton. Geol. Soc. America Bull., v. 98, p. 554-568.

Duebendorfer, E. M., 1988, Evidence for an inverted metamorphic gradient associated with a Precambrian suture, southern Wyoming. Jour. of Metamorphic Geology, v. 6, p. 41-63.

Hattori, K. H., and Cameron, E. M., 2004, Using the High Mobility of Palladium in Surface Media in Exploration for Platinum Group Element Deposits: Evidence from the Lac des Iles Region, Northwestern Ontario. Economic Geology, v. 99, p. 157-171.

Hausel, W. D., and Sutherland, W. M., 2005, Preliminary Geologic Map of the Keystone Quadrangle, Albany and Carbon Counties, Wyoming. Open File Report 05-6, Keystone 1:24,000 – Scale Geologic Map.

Hedge, C. E., Peterman, Z. E., and Braddock, W. A., 1967, Age of the major Precambrian regional metamorphism in the northern Front Range, Colorado. Geol. Soc. America Bull., v. 78, p. 551-557.

Hills, F. A., Gast, P. W., Houston, R. S., and Swainbank, I. G., 1968, Precambrian geochronology of the Medicine Bow Mountains, southeastern Wyoming. Geol. Soc. America Bull., v. 79, p. 1757-1783.

Jones, D. S., Snoke, A. W., and Chamberlain, W. R., 2010, New models for Paleoproterozoic orogenesis in the Cheyenne belt region: Evidence from the geology and U-Pb geochronology of the Big Creek Gneiss, southeastern Wyoming. Geol. Soc. America Bull., v. 122, p. 1877-1898.

Houston, R. S., and others, 1968, A regional study of rocks of Precambrian age in that part of the Medicine Bow Mountains lying in southeastern Wyoming. Wyoming Geol. Survey Mem. 1.

Karlstrom, K.A., and Houston, R.A., 1984, The Cheyenne Belt: Analysis of a Proterozoic suture in southern Wyoming. Precambrian Research, v. 25, p. 415-446.

Kasteler, J. I., and Frey, E., 1949, Diamond drilling at the Rambler copper mine, Albany County, Wyo. U.S. Bur. Mines Rept. Inv. 4544.

Kemp, J. F., 1904, Platinum in the Rambler mine, Wyoming. U.S. Geol. Survey Mineral Resources of the U.S., 1902, p. 244-250.

McCallum, M. E., 1974, Dedolomitized marble lenses in shear zone tectonites, Medicine Bow Mountains, Wyoming. Jour. Geology, v. 82, p. 473-487.

McCallum, M. E., Loucks, R. R., Carlson, R. R., Cooley, E. F., and Doerge, T. A., 1976, Platinum Metals Associated with Hydrothermal Copper Ores of the New Rambler Mine, Medicine Bow Mountains, Wyoming. Economic Geology, v. 71, p. 1429 – 1450.

Mountain, B. W., and Wood, S. A., 1988, Chemical Controls on the Solubility, Transport, and Deposition of Platinum and Palladium in Hydrothermal Solutions: A Thermodynamic Approach. Economic Geology, v. 83, p. 492-510.

Orback, C. J., 1958, Geology of the New Rambler mine area, Albany County, Wyoming. Wyoming Geol. Survey open file rept.

Pebesma, E.J., 2004. Multivariable geostatistics in S: the gstat package. Computers & Geosciences, 30: 683-691.

Pebesma, E., and Bivand, R., 2005, Classes and methods for spatial data in R. _R News_,*5*(2), 9-13. <https://CRAN.R-project.org/doc/Rnews/>

Pebesma, E., and Bivand, R., 2023, Spatial Data Science: With Applications in R. Chapman and Hall/CRC. https://doi.org/10.1201/9780429459016

Strickland, D., Chamberlain, K. R., and Duebendorfer, E. M., 2004, Structural and thermochronologic evidence for a ca. 1.6 Ga contractional event in southeastern Wyoming. Geol. Soc. of America Abstracts with Programs, v. 36, no. 5, p. 405.

Sullivan, W. A., Beane, R. J., Fereday, W. H., and Roberts-Pierel, A. M., 2011, Testing the transpression hypothesis in the western part of the Cheyenne belt, Medicine Bow Mountains, southeastern Wyoming. Rocky Mountain Geol., v. 46, no. 2, p. 111-135.

Theobald, P. K. Jr., and Thompson, C. E., 1969, Platinum and Associated Elements at the New Rambler Mine and Vicinity Albany and Carbon Counties Wyoming. U.S. Geol. Survey Circular 607.

U.S. Bureau of Mines, 1942, Rambler Mine, Albany County, Wyoming. U.S. Bur. Mines War Mineral Rept. 17.

Wei, T., and Simko, W., 2021, R package 'corrplot': Visualization of a Correlation Matrix (Version 0.92). Available from https://github.com/taiyun/corrplot